Journal of Thermal Analysis, Vol. 31 (1986) 1027–1036

KINETIC ANALYSIS OF THERMOGRAVIMETRIC DATA. XXV. DERIVATOGRAPHIC STUDY OF SOME $[Co(NCS)_2(amine)_2]$ TYPE COMPLEXES

*J. Zsakó**, *G. Liptay*** and *Cs. Várhelyi**

*FACULTY OF CHEMICAL TECHNOLOGY, "BABEŞ-BOLYAI UNIVERSITY",
3400–CLUJ-NAPOCA, ROMANIA
**DEPARTMENT OF INORGANIC CHEMISTRY, TECHNICAL UNIVERSITY,
1521–BUDAPEST, HUNGARY

(Received April 23, 1985)

Seven complexes of the type $[Co(NCS)_2(amine)_2]$, where amine = aniline (I), *o*-toluidine (II), *m*-toluidine (III), *p*-toluidine (IV), *m*-xylidine (V), *p*-anisidine (VI) or *p*-phenetidine (VII), have been synthesized, and characterized. Their thermal decompositions have been studied with a derivatograph at different heating rates. The DTA curves show only exothermic peaks for the deamination processes, except in the case of II. The TG curves do not indicate the formation of well-defined, relatively stable intermediates. For several decomposition stages, apparent kinetic parameters have been derived from the TG curves by using a nomogram method. A linear kinetic compensation law is observed. The results are discussed in terms of bond strength, steric hindrance and crystal structure.

The thermal decompositions of a large number of $[MX_2(amine)_2]$ type complexes (M = Ni(II), Co(II), Mn(II), Zn(II), Cd(II) or Cu(II), and X = halide or pseudohalide) have been studied under various conditions [1–6 and references therein]. The common feature of these processes is the release of amine molecules, which occurs in some cases, as with many pyridine derivatives, in accordance with the possible reaction schemes

$$\begin{tikzcd}
 & MX_2py \arrow[dr] \arrow[dd] & \\
MX_2py_2 \arrow[ur] \arrow[dr] & & MX_2py_{2/3} \arrow[dl] \\
 & MX_2 &
\end{tikzcd}$$

Frequently, the stoichiometry of the thermal decomposition is not clear, and the number of moles of amine liberated during the first decomposition stage depends on the working conditions. Thus, in the case of the $[CoX_2(amine)_2]$ type complexes (X = Cl, Br or I) containing aromatic amines, this number showed a systematic decrease with increasing sample weight and heating rate [7]. Since these deamination reactions are exothermic processes [6], the participation of atmospheric oxygen may also be presumed.

John Wiley & Sons, Limited, Chichester
Akadémiai Kiadó, Budapest

In a previous paper [5] the influence of the sample weight and of the heating rate upon the thermal decompositions of $[Co(NCS)_2(amine)_2]$ type complexes with amine = aniline, *p*-toluidine and *m*-toluidine was studied by recording TG curves and by deriving kinetic parameters. The apparent activation energies obtained increased in the sequence aniline < *m*-toluidine < *p*-toluidine. The decomposition temperatures decreased in the same sequence. This anomalous behaviour is presumably correlated with the crystal structures of the complexes and with the steric effects of the substituents.

In the present paper a study was made of the thermal decompositions of seven dithiocyanatodiamino-cobalt(II) complexes, containing aniline or aniline derivatives, at different heating rates.

Experimental

0.1 mole cobalt(II) acetate and 0.2 mole KCNS were dissolved in 300 ml hot water. The solution was kept boiling and treated with 0.15–0.2 mole aromatic amine in a few ml of alcohol. After boiling for 15–90 min (depending on the nature

Table 1 Analytical data on the $[Co(NCS)_2(amine)_2]$ type complexes

Formula	Mol. weight calcd.		Analysis calcd. %	Analysis found %
$[Co(NCS)_2(aniline)_2]$ (I)	361.3	Co	16.31	16.20
		NCS	32.15	31.88
$[Co(NCS)_2(o\text{-toluidine})_2]$ (II)	389.4	Co	15.14	15.00
		NCS	30.04	29.87
$[Co(NCS)_2(m\text{-toluidine})_2]$ (III)	389.4	Co	15.14	15.19
		NCS	30.04	29.77
$[Co(NCS)_2(p\text{-toluidine})_2]$ (IV)	389.4	Co	15.14	15.03
		NCS	30.04	30.15
$[Co(NCS)_2(m\text{-xylidine})_2]$ (V)	417.46	Co	14.12	14.25
		NCS	27.83	27.65
$[Co(NCS)_2(p\text{-anisidine})_2] \cdot 1.5\ H_2O$ (VI)	448.4	Co	13.15	13.45
		NCS	25.91	26.18
$[Co(NCS)_2(p\text{-phenetidine})_2] \cdot 1.5\ H_2O$ (VII)	476.5	Co	12.31	12.70
		NCS	24.38	24.70

(Cobalt was determined complexometrically and thiocyanate as $BaSO_4$)

of the amine), the solution was cooled and the crystalline product formed was filtered, washed with water and dried in air (yield 40–70%). The characterization and analytical data on the complexes are detailed in Table 1.

The thermal decompositions of the complexes were studied with a derivatograph (MOM, Budapest) on samples of 100 mg, at three different heating rates: $q = 1, 2$ and 5 deg/min^{-1}, respectively. The curves were recorded up to 400°.

Results and discussion

Three typical TG and DTA curves are presented in Fig. 1.

It is seen that for the aniline complex(I) all the decomposition stages are exothermic and they begin at relatively high temperatures (Fig. 1a). Similar curves were obtained for complexes III, IV and V. For II (Fig. 1b) the thermal decomposition begins at much lower temperatures. The first stage is quite unusual, showing an endothermic effect initially, but later becoming strongly exothermic. Neither the TG nor the DTG curves show this stage to be complex one; the two peaks mentioned above appear only in the DTA curves. The further decomposition stages are exothermic.

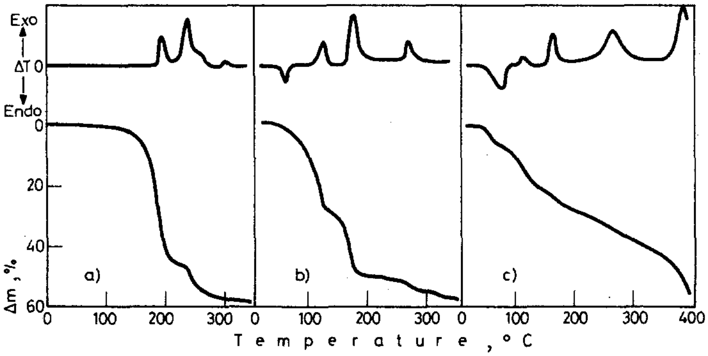

Fig. 1 TG and DTA curves. a = [Co(NCS)$_2$(aniline)$_2$], $q = 1$ deg min^{-1}; b = [Co(NCS)$_2$(*o*-toluidine)$_2$], $q = 2$ deg min^{-1}; c = [Co(NCS)$_2$(*p*-anisidine)$_2$], $q = 1$ deg min^{-1}

The decomposition of VI (Fig. 1c) begins at very low temperatures and the first stage is clearly endothermic. In this stage the crystallization water is lost. The deamination processes are exothermic and the first of them begins at relatively low temperature. Similar curves are obtained with complex VII. The DTA peak temperatures are presented in Table 2.

The deamination reactions occur in 3–4 successive stages. All are exothermic

Table 2 DTA peak temperatures in thermal decomposition of $[Co(NCS)_2(amine)_2]$ type complexes

Complex	q, deg min^{-1}	Endotherm, °C	Exotherm, °C
I	1	—	205, 248, 258, 335
	2	—	215, 255, 267, 340
	5	—	230, 270, 290, 350
II	1	58	100, 175, 240
	2	68	125, 178, 270
	5	70	140, 175, 300
III	1	—	188, 253, 330
	2	—	202, 283, 340
	5	—	215, 298, 365
IV	1	—	185, 197, 335
	2	—	195, 208, 355
	5	—	214, 265, 375
V	1	—	172, 188, 270
	2	—	180, 195, 280
	5	—	180, 202, 315
VI	1	65	110, 162, 265, 395
	2	70	125, 165, 275, 400
	5	77	170, 200, 290, 400
VII	1	62	110, 150, 285, 380
	2	68	120, 158, 295, 400
	5	68	130, 162, 300, 400

processes, suggesting that atmospheric oxygen takes part in these reactions. With increasing heating rate, the DTA peaks are shifted towards higher temperatures. The first exothermic peak temperature diminishes in the following sequence:

$$I > III > IV > V > VI > VII > II$$

indicating the decreasing thermal stability of the complexes.

As concerns the stoichiometry of the deamination reactions, the TG curves do not show the formation of stable intermediates. As seen from the data presented in Table 3, the weight loss in a given decomposition stage is influenced even by the heating rate. Only the release of the crystallization water seems to occur quantitatively, leading to the formation of the relatively stable anhydrous complex salt.

Table 3 Weight losses in the decomposition stages, expressed as numbers of moles of amine, or of water*, respectively

Complex	Stage	q, deg min^{-1}		
		1	2	5
I	1	1.71	1.63	1.48
II	1	0.47	0.98	1.00
	2	1.28	0.84	0.53
III	1	1.24	1.20	1.02
IV	1	1.02	0.98	0.95
V	1	0.72	0.62	0.55
VI	1	1.49*	1.48*	1.48*
	2	0.58	0.58	0.66
VII	1	1.48*	1.48*	1.32*
	2	0.43	0.54	0.54

The thermal decompositions involve not only deamination reactions, but also redox processes. This is indicated by the exothermic character of the reactions, and also by the total weight losses up to 400°.

As seen from Table 4, in some cases the ratio of the sample weight to the $Co(NCS)_2$ content of the sample at 400° is less than unity. The TG curves in these cases show no weight loss stop corresponding to the formation of $Co(NCS)_2$. Thus, the decomposition is very complex and may involve not only the release of amine molecules, but also the oxidation of the amine, of the NCS^- ions, and of Co(II) to Co(III).

The shape of the TG curves allows the derivation of kinetic parameters for several decomposition stages. Such stages are the dehydration reactions, the first stage of the deamination and also the second deamination stage of II.

Table 4 Ratio of sample weight at 400° to $Co(NCS)_2$ content

Complex	q, deg min^{-1}		
	1	2	5
I	0.825	0.928	1.010
II	0.867	0.889	0.956
III	1.156	1.178	1.267
IV	1.244	1.356	1.289
V	1.364	1.317	1.294
VI	1.151	1.381	1.355
VII	1.549	1.495	1.359

In order to derive the kinetic parameters, viz. the apparent reaction order (n), the activation energy (E) and the pre-exponential factor (Z, s^{-1}), our nomogram method [8] was used, as well as the interpolation curve proposed earlier [9]. The results are presented in Tables 5–7. These Tables also contain the reduced position parameter τ^*, correlated with the position parameter

$$\tau = 10^3 T_{0.1}^{-1}$$

where $T_{0.1}$ is the temperature at which the transformation degree in the given stage is equal to $\alpha = 0.1$.

Table 5 Kinetic parameters of the dehydration reactions (323 K $< T_{0.1} <$ 338 K)

Complex	q, deg min^{-1}	n	E, kJ mole^{-1}	log Z	τ^*
VI	1	0.07	138.9	19.0	2.960
	2	0.57	137.5	19.1	2.994
	5	0.71	104,2	13.9	3.027
VII	1	0.75	148.7	21.3	3.042
	2	0.61	170.0	24.4	3.021
	5	1.06	160.3	23.0	3.083
VI	mean	0.45	126.9	17.3	2.994
VII	mean	0.81	159.7	22.9	3.049
overall	mean	0.63	143.3	20.1	3.021

Table 6 Kinetic parameters of the low-temperature deamination reactions (370 K $< T_{0.1} <$ 395 K)

Complex	q, deg min^{-1}	n	E, kJ mole^{-1}	log Z	τ^*
II	1	−0.06	49.1	3.5	2.700
	2	0.36	59.7	5.1	2.627
	5	0.34	55.2	4.6	2.662
VI	1	1.24	72.3	6.5	2.529
	2	1.33	76.2	7.2	2.568
	5	0.92	62.7	5.2	2.532
VII	1	1.11	78.7	7.5	2.555
	2	1.41	68.7	6.1	2.530
	5	0.64	55.6	4.3	2.570
II	mean values	0.21	54.7	4.4	2.663
VI		1.16	70.4	6.3	2.543
VII		1.05	67.7	6.0	2.552
overall	mean	0.81	64.3	5.6	2.586

Table 7 Kinetic parameters of the high-temperature deamination reactions (433 K $< T_{0.1} <$ 476 K)

Complex	q, deg min^{-1}	n	E, kJ mole^{-1}	log Z	τ^*
I	1	0.30	114.2	10.0	2.104
	2	0.23	98.2	7.9	2.113
	5	0.04	100.3	8.4	2.125
II	1	0.05	85.5	6.8	2.205
	2	0.13	113.3	10.5	2.263
	5	0.41	160.4	15.6	2.309
III	1	0.15	109.8	9.3	2.145
	2	0.23	92.8	7.4	2.154
	5	0.30	110.6	9.7	2.184
IV	1	0.29	109.6	9.4	2.177
	2	0.09	106.9	9.1	2.169
	5	0.29	101.4	8.6	2.195
V	1	−0.10	81.1	6.2	2.200
	2	0.01	93.1	7.9	2.240
	5	0.09	94.2	8.2	2.274
I	mean values	0.19	104.2	8.8	2.117
II		0.16	119.7	11.0	2.259
III		0.23	104.4	8.8	2.161
IV		0.22	106.0	9.0	2.180
V		0.00	89.4	7.4	2.238
overall	mean	0.16	104.7	9.0	2.191

The influence of the heating rate upon the kinetic parameters does not present a uniform picture, but the E values always vary in the same direction as log Z. The mean value of the apparent activation energy of the first deamination stage decreases in the sequence:

$$\mathrm{IV} > \mathrm{III} > \mathrm{I} > \mathrm{V} > \mathrm{VI} > \mathrm{VII} > \mathrm{II}$$

This sequence is almost the same as the sequence of the DTA peak temperatures. An inversion is observed only at the beginning of this series, and this is in full agreement with our earlier results [5].

The graphical plot of log Z vs. E shows the validity of the linear kinetic compensation law

$$\log Z = aE + b$$

All the E and log Z values derived in this paper give three distinct straight lines:

one for the dehydration reactions (Table 5), one for the low-temperature deamination processes (Table 6), and one for the high-temperature deaminations (Table 7).

The parameters a and b of these straight lines were derived by means of the least square method, and are given in Table 8. The same Table contains Jaffé's correlation coefficient ϱ [10], the mean values of τ^* and of E, as well as the magnitude $a' = (2.303\ RT_{0.1})^{-1}$.

Table 8 Kinetic compensation parameters

Reaction		τ^*	a mole/kJ	b	ϱ	a'	$\bar{E}$, kJ/mole
dehydration		3.021	0.1621	−3.11	0.9979	0.1578	143.3
low-temperature deamination		2.586	0.1313	−2.88	0.9953	0.1351	64.2
high-temperature deamination		2.191	0.1176	−3.32	0.9938	0.1144	104.8
deamination of IV							
	1	2.226	0.1073	−2.39	0.9865	0.1163	88.1
	2	2.217	0.1080	−2.45	0.9902	0.1158	91.7
deamination of III							
	1	2.210	0.1169	−3.25	0.9936	0.1155	82.3
	2	2.200	0.1157	−3.18	0.9944	0.1149	86.7
deamination of I							
	1	2.171	0.1174	−3.43	0.9951	0.1135	78.2
	2	2.160	0.1172	−3.42	0.9963	0.1128	83.4

The calculation of a' is of some interest, since according to Garn [11] the kinetic compensation effect is an apparent one, and the above linear kinetic compensation law is a consequence of the use of the Arrhenius equation. Thus, if several decomposition reactions occur in a relatively narrow temperature range, there will be to a first approximation a common isokinetic temperature T_c. In this case a log Z vs. E plot will give a straight line, with slope $(2.303\ RT_c)^{-1}$.

As seen from the first three lines in Table 8, the log Z vs. E plots exhibit a very good linearity ($\varrho > 0.99$) and the slopes are mainly determined by the temperature interval of the thermal decomposition, as presumed by Garn, i.e. the a and a' values are quite close to each other.

In order to verify the compatibility of the kinetic parameters obtained in the present paper for I, III and IV with those reported earlier [5], log Z vs. E plots were produced by using separately for each complex all the values obtained both in the present paper and in [5]. The results are presented in line *2* in Table 8. The kinetic and compensation parameters given in line *1* were taken from [5].

The kinetic parameters derived in the present paper are seen to be in good agreement with those reported earlier.

The incorporation of the new data in the set of kinetic parameters previously derived does not influence the values of the compensation parameters essentially, and it even leads to an increase of ϱ. This result seems to be important, since in our previous work the TG curves were not obtained with a derivatograph, but with a simple thermobalance.

The mean value of the apparent activation energy becomes higher due to the new data, which is not surprising, since in the present paper much lower heating rates were used than before (1, 2 and 5 deg $\min^{-1}$ instead of 5, 10 and 15 deg $\min^{-1}$), and the apparent activation energy generally decreases with increasing heating rate. The new mean values decrease in the same sequence as reported earlier, i.e. IV > III > I.

The same sequence is observed for a', but exactly the reverse for a. This is in contradiction with Garn's hypothesis, but it is in agreement with our presumption [12] postulating that the higher the strength of the chemical bond to be broken, the lower the parameter a will be. The bond strength is mainly determined by the nucleophilic character of the amine, which increases in the sequence aniline < *m*-toluidine < *p*-toluidine, and thus the Co-amine bond strength must increase in the same sequence. Our results show that both the mean E value and the compensation parameter a are determined by this bond strength for these three complexes.

The thermal stability, characterized by the decomposition temperature or by the position parameter τ, is not determined only by the bond strength, but also by the stability of the crystal lattice. IR spectral and magnetic susceptibility data show the complexes $[Co(NCS)_2(amine)_2]$ to have a distorted octahedral structure with NCS bridges [5, 13]. A CH_3 substituent on the aromatic ring strengthens the Co-amine bond, but it reduces the stability of the crystal lattice through steric hindrance.

In the case of *o*-toluidine, even the Co-amine bond strength is reduced by steric hindrance. Therefore, both the thermal stability and the apparent activation energy of the first deamination step are less in the case of II.

On the basis of Hammett's σ constant for the substituents of aniline [14], the Co-amine bond can be expected to be the strongest for VI and VII. Nevertheless, the mean E value of the first deamination stage is lower than for I, III, IV and V. Complexes VI and VII also contain crystallization water, which can be considered to be linked to the O atom of the amine, presumably via H-bonds. Thus, an enhanced steric effect of the substituent appears in the initial crystal lattice. The loss of the crystallization water leads to fragmentation of the crystals and to a loose structure allowing the almost free diffusion of the gaseous products evolved. Therefore, the first deamination stage begins at lower temperature than for I, III, IV or V. Under these conditions, the low apparent activation energy values are not surprising, since a parallelism between E and the bond strength can be expected only if the crystal structure and the particle size are almost the same.

References

1 J. R. Allan, D. H. Brown, R. H. Nuttal and D. W. A. Sharp, J. Inorg. Nucl. Chem., 27 (1965) 1529.

2 G. Belach, C. T. Mortimer and E. G. Tyler, J. Chem. Soc. A. (1967) 1111; (1969) 512.

3 I. G. Murgulescu, E. Segal and D. Fătu, J. Thermal Anal., 1 (1969) 67.

4 G. Liptay, K. Burger, E. Mocsári-Fülöp and I. Porubszky, J. Thermal Anal., 2 (1970) 25.

5 J. Zsakó, Cs. Várhelyi, B. Csegedi and J. Zsakó jr., Thermochim. Acta, 45 (1981) 11.

6 J. Zsakó, G. Liptay, Cs. Várhelyi and E. Brandt-Petrik, Polish J. Chem., in press.

7 J. Zsakó, E. Kékedy and Cs. Várhelyi, Thermal Analysis, Proc. 3rd ICTA, Vol. 2. Davos, Schwitzerland, 1971, p. 487.

8 J. Zsakó, J. Thermal Anal., 15 (1979) 369.

9 J. Zsakó, M. Várhelyi and Cs. Várhelyi, J. Thermal Anal., 17 (1979) 123.

10 H. H. Jaffé, Chem. Rev., 53 (1953) 191.

11 P. D. Garn, J. Thermal Anal., 7 (1975) 475; 10 (1976) 99.

12 J. Zsakó, Cs. Várhelyi, G. Liptay and K. Szilágyi, J. Thermal Anal., 7 (1975) 41.

13 G. Liptay, Thermochim. Acta, 15 (1976) 159.

14 J. Hine, Physical Organic Chemistry, McGraw-Hill, New York, 1956, p. 72.

Zusammenfassung — Sieben Komplexe des Typs $[Co(NCS)_2(amin)_2]$ (amin = Anilin, *o*-Toluidin, *m*-Toluidin, *p*-Toluidin, *m*-Xylidin, *p*-Anisidin und *p*-Phenetidin) wurden dargestellt und charakterisiert. Die thermische Zersetzung dieser Komplexe wurde derivatographisch bei verschiedenen Aufheizgeschwindigkeiten untersucht. Mit Ausnahme von *o*-Toluidin weisen die DTA-Kurven bei allen Komplexen nur exotherme Peaks für den Deaminierungsprozeß auf. Die TG-Kurven geben keine Hinweise auf die Bildung gut definierter, relativ stabiler Zwischenprodukte. Für einige Phasen der Zersetzung werden aus den TG-Kurven nach einer Nomogramm-Methode scheinbare kinetische Parameter berechnet. Es wurde ein lineares kinetisches Kompensationsgesetz beobachtet. Die Ergebnisse werden im Hinblick auf Bindungsstärken, sterische Hinderungen und die Kristallstruktur diskutiert.

Резюме — Синтезированы и охарактеризованы семь комплексов общей формулы $[Co(амин)_2(NCS)_2]$, где амин = анилип (I), *о*-толуидин (II), *м*-толуидин (III), *n*-толуидин (IV), *м*-ксилидин (V), *n*-анизидин (VI) и *n*-фенетидин (VII). Термическое повеnение их при различных скоростях нагрева исследовано с помощью дериватографа. ДТА кривые соединений, за исключением соединения II, показали только экзотермические пики процессов деаминирования. Кривые ТГ не показали образования каких-либо относительно устойчивых промежуточных продуктов. Используя метод номограм, на основе кривых ТГ установлены кажущиеся кинетические параметры некоторых стадий разложения. Разложение комплексов подчиняется линейнаму кинетическому компенсационному закону. Полученные результаты обсуждены на основе энергий связи, стерических препятствий и кристаллической структуры исследованных комплексов.